CLEO CONF 98-20
ICHEP98 858

First observation of the decay $B^{\pm} \to K^{\pm}\pi^{0}$

CLEO Collaboration

(July 21, 1998)

Abstract

We have studied two-body charmless hadronic decays of B mesons into the final states $h^{+}h^{-}$, $h^{\pm}K^{0}_{S}$, and $h^{\pm}\pi^{0}$, where $h^{\pm}$ stands for a charged kaon or pion. We present preliminary results based on nearly 6 million $B\bar{B}$ pairs collected with the CLEO II and CLEO II.5 detectors. We have made the first observation of the decay $B^{\pm} \to K^{\pm}\pi^{0}$, with the branching fraction of $Br(B^{\pm} \to K^{\pm}\pi^{0}) = (1.5 \pm 0.4 \pm 0.3) \times 10^{-5}$. We have also measured $Br(B \to K^{\pm}\pi^{\mp}) = (1.4 \pm 0.3 \pm 0.2) \times 10^{-5}$ and $Br(B^{\pm} \to K^{0}\pi^{\pm}) = (1.4 \pm 0.5 \pm 0.2) \times 10^{-5}$, confirming our previously published results. We see no significant signal in $B \to \pi^{+}\pi^{-}$, and set an upper limit of $Br(B \to \pi^{+}\pi^{-}) < 8.4 \times 10^{-6}$ at 90% confidence level.

M. Artuso,[1] E. Dambasuren,[1] S. Kopp,[1] G. C. Moneti,[1] R. Mountain,[1] S. Schuh,[1] T. Skwarnicki,[1] S. Stone,[1] A. Titov,[1] G. Viehhauser,[1] J.C. Wang,[1] J. Bartelt,[2] S. E. Csorna,[2] K. W. McLean,[2] S. Marka,[2] Z. Xu,[2] R. Godang,[3] K. Kinoshita,[3] I. C. Lai,[3] P. Pomianowski,[3] S. Schrenk,[3] G. Bonvicini,[4] D. Cinabro,[4] R. Greene,[4] L. P. Perera,[4] G. J. Zhou,[4] S. Chan,[5] G. Eigen,[5] E. Lipeles,[5] J. S. Miller,[5] M. Schmidtler,[5] A. Shapiro,[5] W. M. Sun,[5] J. Urheim,[5] A. J. Weinstein,[5] F. Würthwein,[5] D. E. Jaffe,[6] G. Masek,[6] H. P. Paar,[6] E. M. Potter,[6] S. Prell,[6] V. Sharma,[6] D. M. Asner,[7] J. Gronberg,[7] T. S. Hill,[7] D. J. Lange,[7] R. J. Morrison,[7] T. K. Nelson,[7] D. Roberts,[7] B. H. Behrens,[8] W. T. Ford,[8] A. Gritsan,[8] H. Krieg,[8] J. Roy,[8] J. G. Smith,[8] J. P. Alexander,[9] R. Baker,[9] C. Bebek,[9] B. E. Berger,[9] K. Berkelman,[9] V. Boisvert,[9] D. G. Cassel,[9] D. S. Crowcroft,[9] M. Dickson,[9] S. von Dombrowski,[9] P. S. Drell,[9] K. M. Ecklund,[9] R. Ehrlich,[9] A. D. Foland,[9] P. Gaidarev,[9] R. S. Galik,[9] L. Gibbons,[9] B. Gittelman,[9] S. W. Gray,[9] D. L. Hartill,[9] B. K. Heltsley,[9] P. I. Hopman,[9] J. Kandaswamy,[9] D. L. Kreinick,[9] T. Lee,[9] Y. Liu,[9] N. B. Mistry,[9] C. R. Ng,[9] E. Nordberg,[9] M. Ogg,[9,*] J. R. Patterson,[9] D. Peterson,[9] D. Riley,[9] A. Soffer,[9] B. Valant-Spaight,[9] A. Warburton,[9] C. Ward,[9] M. Athanas,[10] P. Avery,[10] C. D. Jones,[10] M. Lohner,[10] C. Prescott,[10] A. I. Rubiera,[10] J. Yelton,[10] J. Zheng,[10] G. Brandenburg,[11] R. A. Briere,[11] A. Ershov,[11] Y. S. Gao,[11] D. Y.-J. Kim,[11] R. Wilson,[11] H. Yamamoto,[11] T. E. Browder,[12] Y. Li,[12] J. L. Rodriguez,[12] S. K. Sahu,[12] T. Bergfeld,[13] B. I. Eisenstein,[13] J. Ernst,[13] G. E. Gladding,[13] G. D. Gollin,[13] R. M. Hans,[13] E. Johnson,[13] I. Karliner,[13] M. A. Marsh,[13] M. Palmer,[13] M. Selen,[13] J. J. Thaler,[13] K. W. Edwards,[14] A. Bellerive,[15] R. Janicek,[15] P. M. Patel,[15] A. J. Sadoff,[16] R. Ammar,[17] P. Baringer,[17] A. Bean,[17] D. Besson,[17] D. Coppage,[17] C. Darling,[17] R. Davis,[17] S. Kotov,[17] I. Kravchenko,[17] N. Kwak,[17] L. Zhou,[17] S. Anderson,[18] Y. Kubota,[18] S. J. Lee,[18] R. Mahapatra,[18] J. J. O'Neill,[18] R. Poling,[18] T. Riehle,[18] A. Smith,[18] M. S. Alam,[19] S. B. Athar,[19] Z. Ling,[19] A. H. Mahmood,[19] S. Timm,[19] F. Wappler,[19] A. Anastassov,[20] J. E. Duboscq,[20] K. K. Gan,[20] T. Hart,[20] K. Honscheid,[20] H. Kagan,[20] R. Kass,[20] J. Lee,[20] H. Schwarthoff,[20] A. Wolf,[20] M. M. Zoeller,[20] S. J. Richichi,[21] H. Severini,[21] P. Skubic,[21] A. Undrus,[21] M. Bishai,[22] S. Chen,[22] J. Fast,[22] J. W. Hinson,[22] N. Menon,[22] D. H. Miller,[22] E. I. Shibata,[22] I. P. J. Shipsey,[22] S. Glenn,[23] Y. Kwon,[23,†] A.L. Lyon,[23] S. Roberts,[23] E. H. Thorndike,[23] C. P. Jessop,[24] K. Lingel,[24] H. Marsiske,[24] M. L. Perl,[24] V. Savinov,[24] D. Ugolini,[24] X. Zhou,[24] T. E. Coan,[25] V. Fadeyev,[25] I. Korolkov,[25] Y. Maravin,[25] I. Narsky,[25] R. Stroynowski,[25] J. Ye,[25] and T. Wlodek[25]

[1]Syracuse University, Syracuse, New York 13244
[2]Vanderbilt University, Nashville, Tennessee 37235
[3]Virginia Polytechnic Institute and State University, Blacksburg, Virginia 24061
[4]Wayne State University, Detroit, Michigan 48202
[5]California Institute of Technology, Pasadena, California 91125
[6]University of California, San Diego, La Jolla, California 92093
[7]University of California, Santa Barbara, California 93106

[*]Permanent address: University of Texas, Austin TX 78712.

[†]Permanent address: Yonsei University, Seoul 120-749, Korea.

[8]University of Colorado, Boulder, Colorado 80309-0390
[9]Cornell University, Ithaca, New York 14853
[10]University of Florida, Gainesville, Florida 32611
[11]Harvard University, Cambridge, Massachusetts 02138
[12]University of Hawaii at Manoa, Honolulu, Hawaii 96822
[13]University of Illinois, Urbana-Champaign, Illinois 61801
[14]Carleton University, Ottawa, Ontario, Canada K1S 5B6
and the Institute of Particle Physics, Canada
[15]McGill University, Montréal, Québec, Canada H3A 2T8
and the Institute of Particle Physics, Canada
[16]Ithaca College, Ithaca, New York 14850
[17]University of Kansas, Lawrence, Kansas 66045
[18]University of Minnesota, Minneapolis, Minnesota 55455
[19]State University of New York at Albany, Albany, New York 12222
[20]Ohio State University, Columbus, Ohio 43210
[21]University of Oklahoma, Norman, Oklahoma 73019
[22]Purdue University, West Lafayette, Indiana 47907
[23]University of Rochester, Rochester, New York 14627
[24]Stanford Linear Accelerator Center, Stanford University, Stanford, California 94309
[25]Southern Methodist University, Dallas, Texas 75275

The phenomenon of CP violation, so far observed only in the neutral kaon system, can be accommodated by a complex phase in the Cabibbo-Kobayashi-Maskawa (CKM) quark-mixing matrix [1]. Whether this phase is the correct, or only, source of CP violation awaits experimental confirmation. B meson decays, in particular charmless B meson decays, will play an important role in verifying this picture.

The decay $B \to \pi^+\pi^-$, dominated by the $b \to u$ tree diagram (Fig. 1(a)), can be used to measure CP violation due to $B^0 - \bar{B}^0$ mixing at both asymmetric B factories and hadron colliders. However, theoretical uncertainties due to the presence of the $b \to dg$ penguin diagram (Fig. 1(b)) make it difficult to extract the angle α of the unitarity triangle from $B \to \pi^+\pi^-$ alone. Additional measurements of $B^\pm \to \pi^\pm\pi^0$, $B, \bar{B} \to \pi^0\pi^0$, and the use of isospin symmetry may resolve these uncertainties [2].

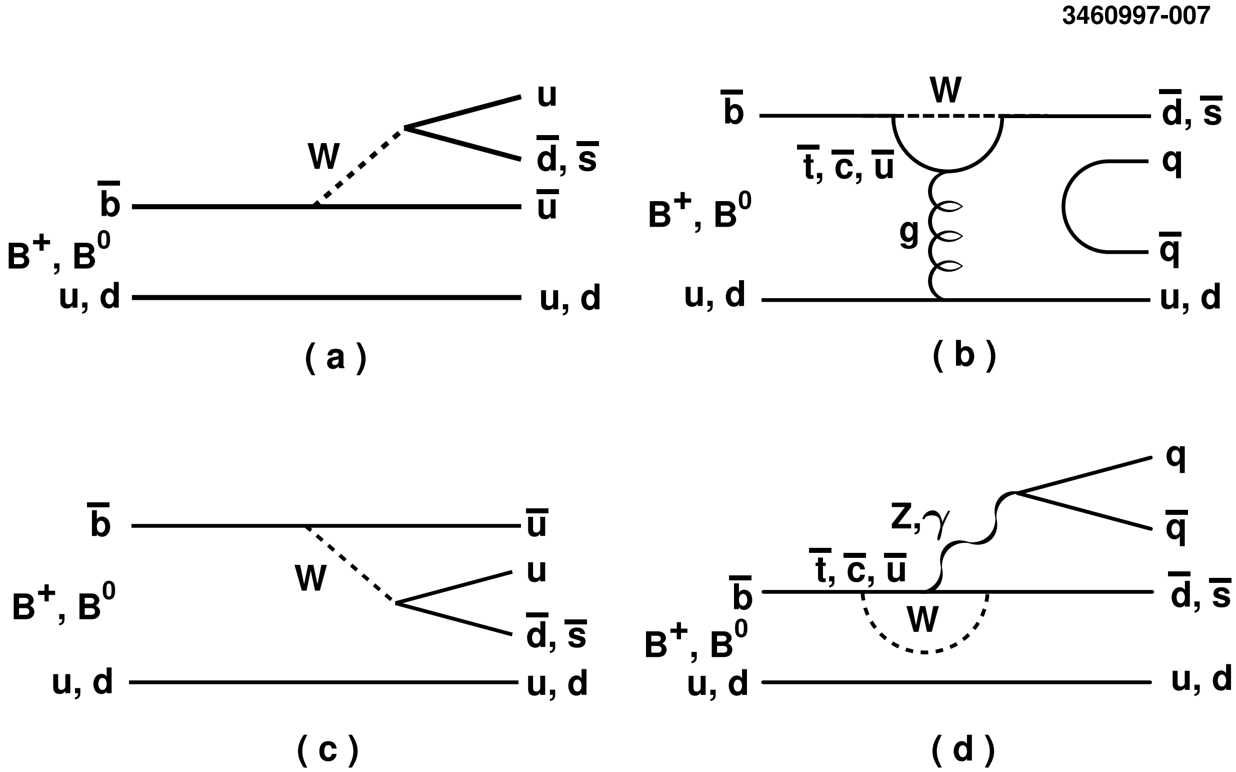

FIG. 1. The dominant decay processes are expected to be (a) external W-emission, (b) gluonic penguin, (c) internal W-emission, (d) external electroweak penguin.

$B \to K\pi$ decays are dominated by the $b \to sg$ gluonic penguin diagram, with additional contributions from $b \to u$ tree and color-allowed electroweak penguin (Fig. 1(d)) processes. Interference between the penguin and spectator amplitudes can lead to direct CP violation, which would manifest itself as a rate asymmetry for decays of B and $\bar{B}$ mesons. Several methods of measuring γ, the phase of V_{ub}. using only decay rates of $B \to K\pi$, $\pi\pi$ processes were also proposed [3]. This is particularly important, as γ is the least known parameter of the unitarity triangle and is likely to remain the most difficult to determine experimentally. The ratio $R = \mathcal{B}(B \to K^\pm\pi^\mp)/\mathcal{B}(B^\pm \to K^0\pi^\pm)$, was recently suggested [4] as a way to constrain γ. However, final state interactions(FSI) in $B \to K\pi$ decays can significantly affect this method [5]. Studies of B decays to the KK final states can provide useful limits on the FSI effects [6]. This paper presents the first observation of the decay $B^\pm \to K^\pm\pi^0$, improved measurements for $B \to K^\pm\pi^\mp$ and $B^\pm \to K^0\pi^\pm$ decays, and updated upper limits for B decays to $\pi^+\pi^-$, $\pi^\pm\pi^0$, K^+K^-, and $K^0K^\pm$.

The data set used in this analysis was collected with the CLEO II and CLEO II.5 detectors at the Cornell Electron Storage Ring (CESR). It consists of 5.6 fb^{-1} taken at the $\Upsilon(4S)$ (on-resonance) and 2.9 fb^{-1} taken below $B\bar{B}$ threshold. The below-threshold sample is used for continuum background studies. The on-resonance sample contains 5.8 million $B\bar{B}$ pairs. This is an 80% increase in the number of $B\bar{B}$ pairs over the published analysis [7]. In addition, we have re-analyzed the CLEO II data set with improved calibration constants and track-fitting algorithm allowing us to extend our geometric acceptance and track quality requirements. This has lead to an overall increase in reconstruction efficiency of $10 - 20$ % as compared to the previously published analysis.

CLEO II and CLEO II.5 are general purpose solenoidal magnet detectors, described in detail elsewhere [8]. In CLEO II, the momenta of charged particles are measured in a tracking system consisting of a 6-layer straw tube chamber, a 10-layer precision drift chamber, and a 51-layer main drift chamber, all operating inside a 1.5 T superconducting solenoid. The main drift chamber also provides a measurement of the specific ionization loss, dE/dx, used for particle identification. For CLEO II.5 the 6-layer straw tube chamber was replaced by a 3-layer double sided silicon vertex detector, and the gas in the main drift chamber was changed from an argon-ethane to a helium-propane mixture. Photons are detected using 7800-crystal CsI(Tl) electromagnetic calorimeter. Muons are identified using proportional counters placed at various depths in the steel return yoke of the magnet.

Charged tracks are required to pass track quality cuts based on the average hit residual and the impact parameters in both the $r - \phi$ and $r - z$ planes. Candidate K^0_S are selected from pairs of tracks forming well measured displaced vertices. Furthermore, we require the K^0_S momentum vector to point back to the beam spot and the $\pi^+\pi^-$ invariant mass to be within 10 MeV, two standard deviations (σ), of the K^0_S mass. Isolated showers with energies greater than 40 MeV in the central region of the CsI calorimeter and greater than 50 MeV elsewhere, are defined to be photons. Pairs of photons with an invariant mass within 25 MeV ($\sim 2.5\sigma$) of the nominal π^0 mass are kinematically fitted with the mass constrained to the π^0 mass. To reduce combinatoric backgrounds we require the lateral shapes of the showers to be consistent with those from photons. To suppress further low energy showers from charged particle interactions in the calorimeter we apply a shower energy dependent isolation cut.

Charged particles are identified as kaons or pions using dE/dx. Electrons are rejected based on dE/dx and the ratio of the track momentum to the associated shower energy in the CsI calorimeter. We reject muons by requiring that the tracks do not penetrate the steel absorber to a depth greater than seven nuclear interaction lengths. We have studied the dE/dx separation between kaons and pions for momenta $p \sim 2.6$ GeV/c in data using D^{*+}-tagged $D^0 \to K^-\pi^+$ decays; we find a separation of (1.7 ± 0.1) σ for CLEO II and (2.0 ± 0.1) σ for CLEO II.5.

We calculate a beam-constrained B mass $M = \sqrt{E_{\rm b}^2 - p_B^2}$, where p_B is the B candidate momentum and $E_{\rm b}$ is the beam energy. The resolution in M ranges from 2.5 to 3.0 MeV/c^2, where the larger resolution corresponds to decay modes with a π^0. We define $\Delta E = E_1 + E_2 - E_{\rm b}$, where E_1 and E_2 are the energies of the daughters of the B meson candidate. The resolution on ΔE is mode-dependent. For final states without π^0's the ΔE resolution for CLEO II(II.5) is $\pm 26(22)$ MeV. In $B^\pm \to h^\pm \pi^0$ analysis ΔE resolution is worse approximately by a factor of two and becomes asymmetric because of energy loss out of the back of the CsI crystals. The energy constraint also helps to distinguish between modes of the same topology. For example, ΔE for $B \to K^+\pi^-$, calculated assuming $B \to \pi^+\pi^-$, has a distribution that is centered at -42 MeV, giving a separation of $1.6(1.9)\sigma$ between $B \to K^+\pi^-$ and $B \to \pi^+\pi^-$ for CLEO II(II.5). We accept events with M within $5.2 - 5.3$ GeV/c^2 and $|\Delta E| < 200(300)$ MeV for decay modes without (with) a π^0 in the final state. This fiducial region includes the signal region, and a sideband for background determination.

We have studied backgrounds from $b \to c$ decays and other $b \to u$ and $b \to s$ decays and find that all are negligible for the analyses presented here. The main background arises from $e^+e^- \to q\bar{q}$ (where $q = u, d, s, c$). Such events typically exhibit a two-jet structure and can produce high momentum back-to-back tracks in the fiducial region. To reduce contamination from these events, we calculate the angle θ_S between the sphericity axis [9] of the candidate tracks and showers and the sphericity axis of the rest of the event. The distribution of $\cos\theta_S$ is strongly peaked at ± 1 for $q\bar{q}$ events and is nearly flat for $B\bar{B}$ events. We require $|\cos\theta_S| < 0.8$ which eliminates 83% of the background. Using a detailed GEANT-based Monte-Carlo simulation [10] we determine overall detection efficiencies ($\mathcal{E}$) of $15 - 53\%$, as listed in Table I. Efficiencies contain branching fractions for $K^0 \to K^0_S \to \pi^+\pi^-$ and $\pi^0 \to \gamma\gamma$ where applicable. We estimate a systematic error on the efficiency using independent data samples.

Additional discrimination between signal and $q\bar{q}$ background is provided by a Fisher discriminant technique as described in detail in Ref. [11]. The Fisher discriminant is a linear combination $\mathcal{F} \equiv \sum_{i=1}^{N} \alpha_i y_i$ where the coefficients α_i are chosen to maximize the separation between the signal and background Monte-Carlo samples. The 11 inputs, y_i, are $|\cos\theta_{cand}|$ (the cosine of the angle between the candidate sphericity axis and beam axis), the ratio of Fox-Wolfram moments H_2/H_0 [12], and nine variables that measure the scalar sum of the momenta of tracks and showers from the rest of the event in nine angular bins, each of 10°, centered about the candidate's sphericity axis.

We perform unbinned maximum-likelihood (ML) fits using ΔE, M, $\mathcal{F}$, $|\cos\theta_B|$ (the angle between the B meson momentum and beam axis), and dE/dx (where applicable) as input information for each candidate event to determine the signal yields. Three different fits are performed, one for each topology (h^+h^-, $h^\pm\pi^0$, and $h^\pm K^0_S$, $h^\pm$ referring to a charged kaon or pion). In each of these fits the likelihood of the event is parameterized by the sum of probabilities for all relevant signal and background hypotheses, with relative weights determined by maximizing the likelihood function ($\mathcal{L}$). The probability of a particular hypothesis is calculated as a product of the probability density functions (PDFs) for each of the input variables. Further details about the likelihood fit can be found in Ref. [11]. The parameters for the PDFs are determined from independent data and high-statistics Monte-Carlo samples. We estimate a systematic error on the fitted yield by varying the PDFs used in the fit within their uncertainties. These uncertainties are dominated by the limited statistics in the independent data samples we used to determine the PDFs. The systematic errors on the measured branching fractions are obtained by adding this fit systematic in quadrature with the systematic error on the efficiency.

Figures 2-4 illustrate contour plots of $-2\ln\mathcal{L}$ for the ML fits to the signal yields (N).

TABLE I. Experimental results and theoretical model predictions [13]. Branching fractions ($\mathcal{B}$) and 90% C.L. upper limits are given in 10^{-5} units. The errors on $\mathcal{B}$ are statistical and systematics respectively. We quote upper limits with (and without) the systematics taken into account. Reconstruction efficiency $\mathcal{E}$ includes branching fractions of $K^0 \to K_S^0 \to \pi^+\pi^-$ and $\pi^0 \to \gamma\gamma$.

Mode	$\mathcal{E}(\%)$	$\mathcal{B}$	Theory $\mathcal{B}$
$\pi^+\pi^-$	53 ± 5	$<\ 0.84(0.66)$	0.8–2.6
$\pi^+\pi^0$	42 ± 4	$<\ 1.6(1.0)$	0.4–2.0
$K^+\pi^-$	53 ± 5	$1.4 \pm 0.3 \pm 0.2$	0.7–2.4
$K^+\pi^0$	42 ± 4	$1.5 \pm 0.4 \pm 0.3$	0.3–1.3
$K^0\pi^+$	15 ± 2	$1.4 \pm 0.5 \pm 0.2$	0.8–1.5
K^+K^-	53 ± 5	$<\ 0.24(0.18)$	–
$K^+\bar{K}^0$	15 ± 2	$<\ 0.93(0.74)$	0.07–0.13

The curves represent the $n\sigma$ contours , which correspond to the increase in $-2\ln\mathcal{L}$ by n^2. The dashed curve marks the 3σ contour and all contour plots do not have systematic errors included. The statistical significance of a given signal yield is determined by repeating the fit with the signal yield fixed to be zero and recording the change in $-2\ln\mathcal{L}$. To further illustrate the fits, Figures 5, 6, and 7 show M (ΔE) projections for events in a signal region defined by $|\Delta E| < 2\sigma_{\Delta E}$ ($|M - 5.28| < 2\sigma_M$) for the final states $K^\pm\pi^\mp$, $K^\pm\pi^0$, and $K_S^0\pi^\pm$. We also make a cut on $\mathcal{F}$ which keeps 67% of the signal and rejects 80% of the background. For Fig. 5 and 6, events are sorted by dE/dx according to the most likely hypothesis. For Fig. 7, 3σ consistency with the pion hypothesis is required. Overlaid on these plots are the projections of the PDFs used in the fit, normalized according to the fit results multiplied by the efficiency of the additional cuts ($\sim 50-70\%$ for the signal and $\sim 1-8\%$ for the background). We find statistically significant signals for the decays $B \to K^\pm\pi^\mp$, $B^\pm \to K^\pm\pi^0$, and $B^\pm \to K_S^0\pi^\pm$.

To evaluate how systematic uncertainties in the PDFs affect the statistical significance of our signals, we repeated the fits for the h^+h^-, $h^\pm\pi^0$, and $h^\pm K_S^0$ modes with all PDFs changed within their uncertainty to maximally reduce the overall signal yield. Under these conditions, the significance of the $K^\pm\pi^\mp$, $K^\pm\pi^0$, and $K_S^0\pi^\pm$ signals becomes 6.7, 4.7, and 4.2 σ respectively.

The fitted yields in the remaining modes are not statistically significant. We calculate 90% confidence level (C.L.) upper limit yields by integrating the likelihood function

$$\frac{\int_0^{N^{UL}} \mathcal{L}_{\max}(N)dN}{\int_0^{\infty} \mathcal{L}_{\max}(N)dN} = 0.90 \tag{1}$$

where $\mathcal{L}_{\max}(N)$ is the maximum $\mathcal{L}$ at fixed N to conservatively account for possible correlations among the free parameters in the fit. We then increase upper limit yields by their systematic errors and reduce detection efficiencies by their systematic errors to calculate branching fraction upper limits given in Table I.

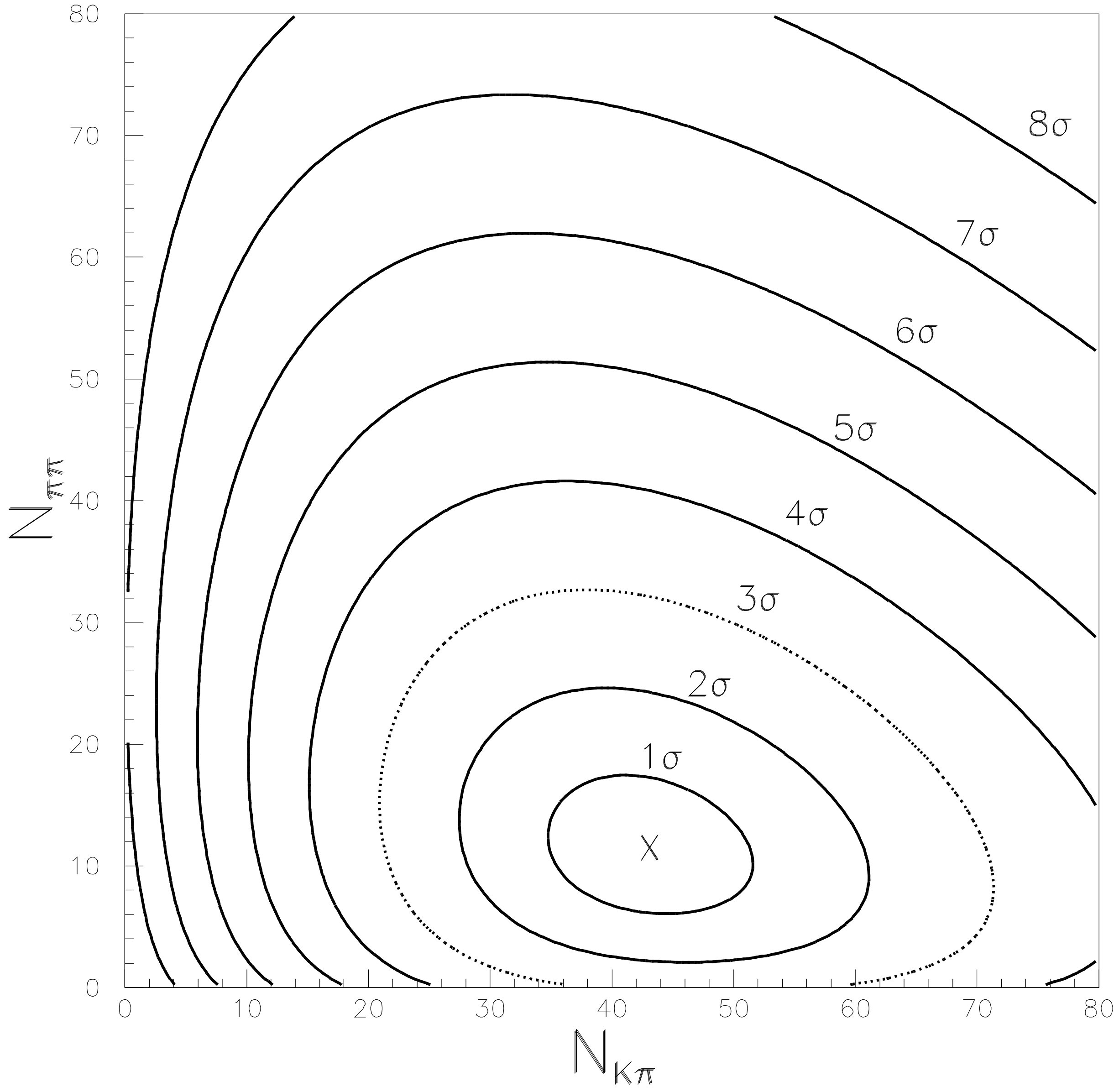

FIG. 2. Contour of the $-2\ln\mathcal{L}$ for the ML fit to $N_{K^{\pm}\pi^{\mp}}$ and $N_{\pi^{+}\pi^{-}}$ for $B \to K^{\pm}\pi^{\mp}$ and $B \to \pi^{+}\pi^{-}$.

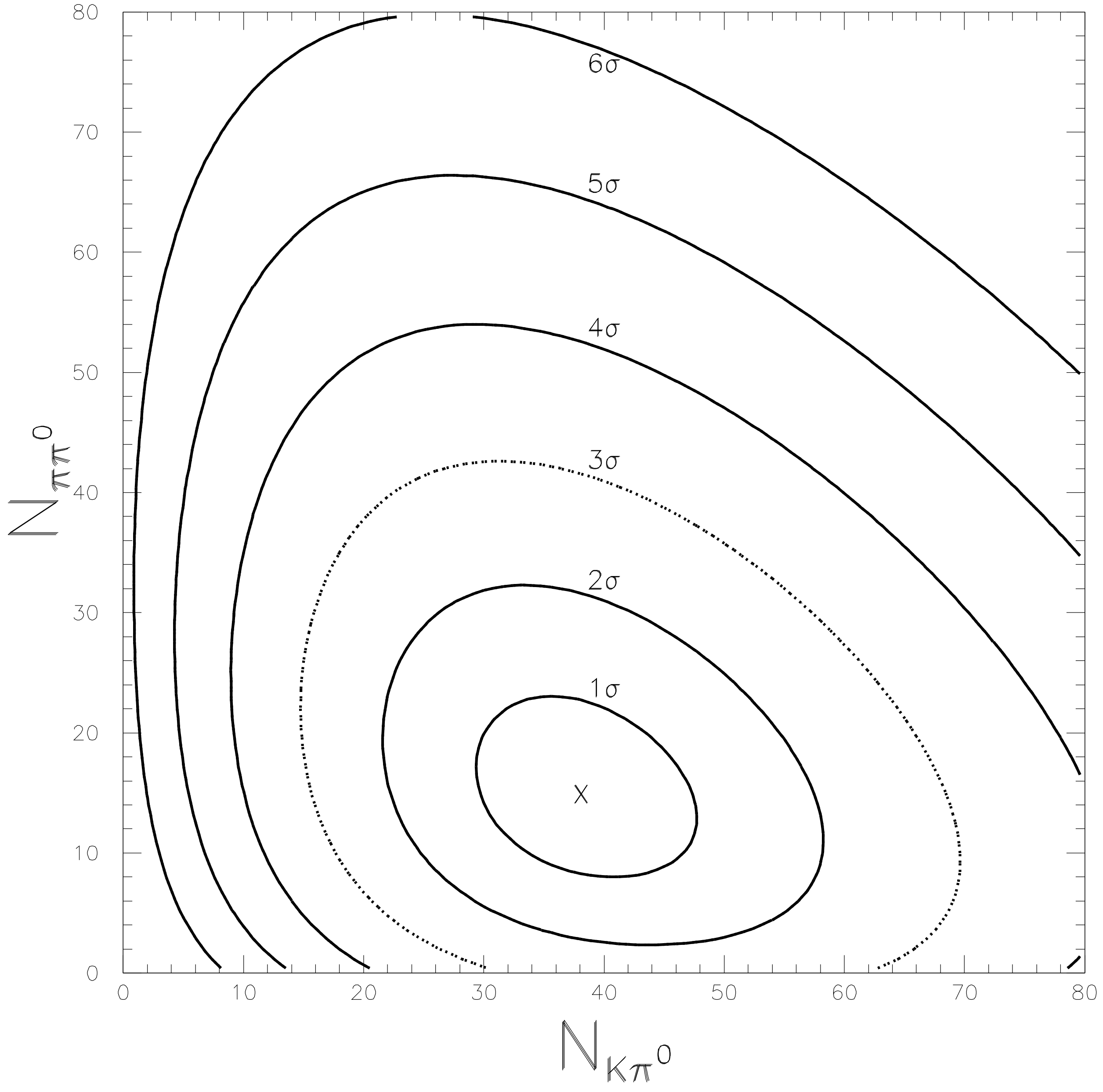

FIG. 3. Contour of the $-2\ln\mathcal{L}$ for the ML fit to $N_{K^\pm\pi^0}$ and $N_{\pi^\pm\pi^0}$ for $B^\pm \to K^\pm\pi^0$ and $B^\pm \to \pi^\pm\pi^0$.

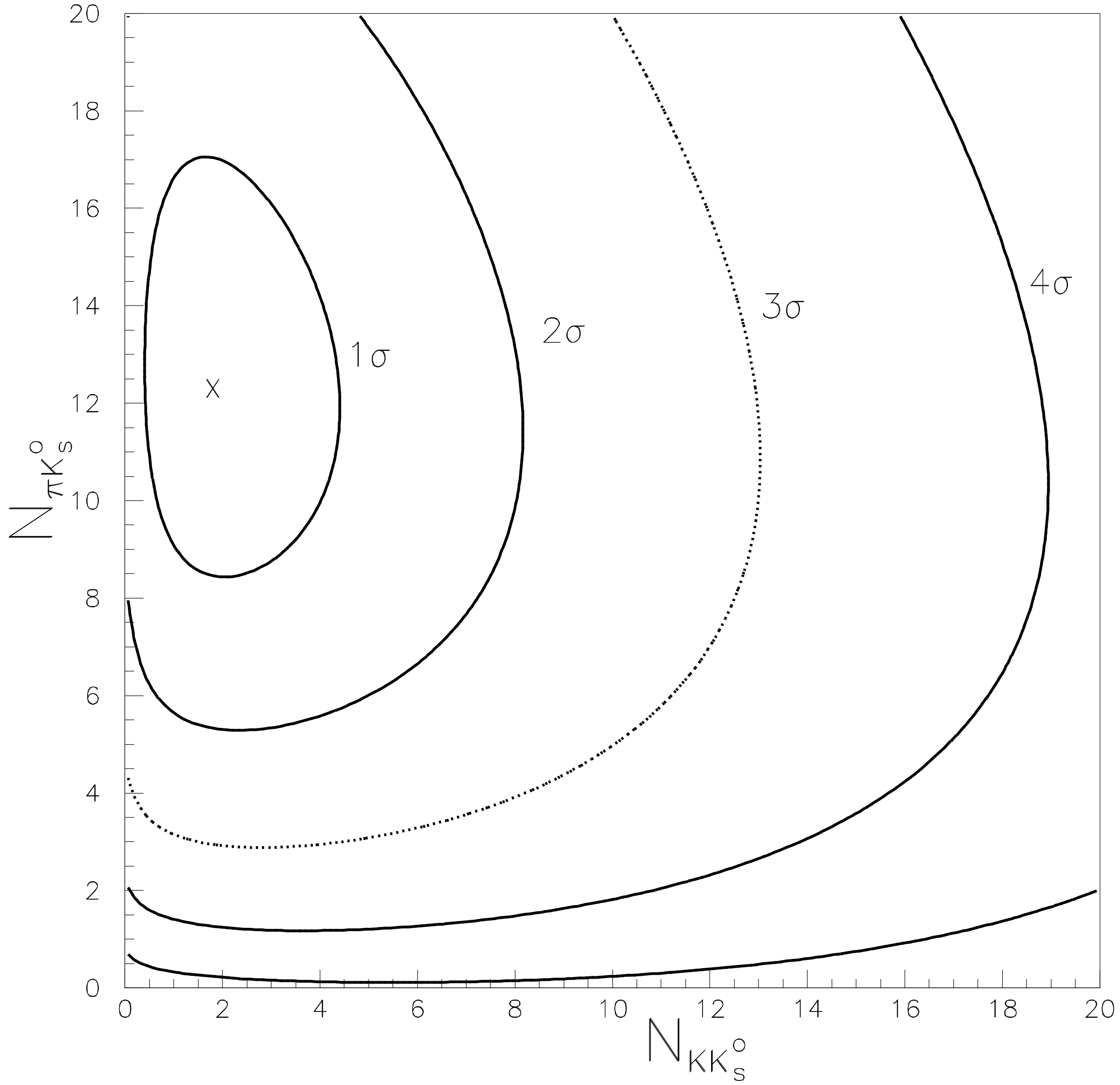

FIG. 4. Contour of the $-2\ln\mathcal{L}$ for the ML fit to $N_{K_S^0\pi^\pm}$ and $N_{K_S^0K^\pm}$ for $B^\pm \to K_S^0\pi^\pm$ and $B^\pm \to K_S^0K^\pm$.

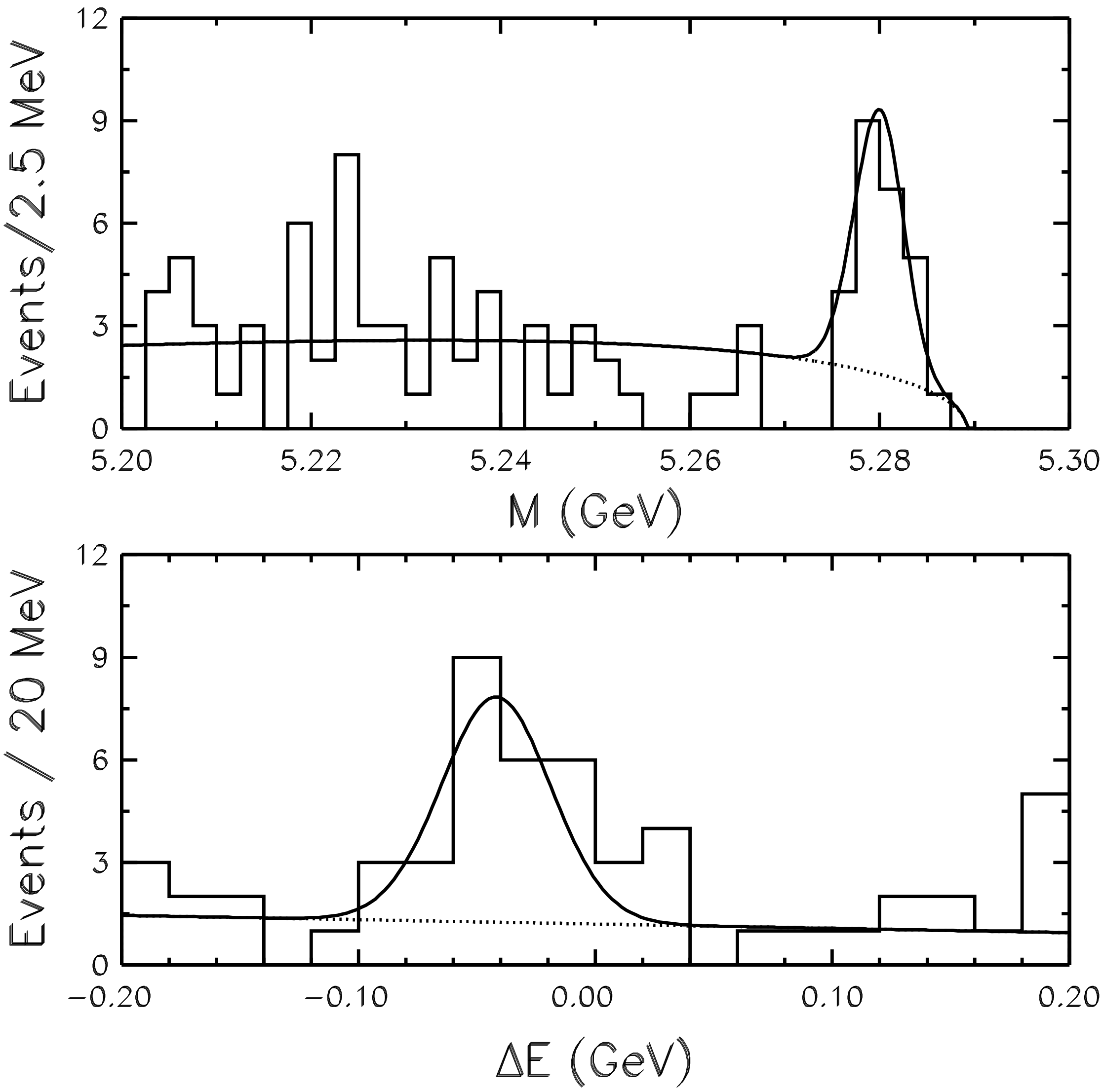

FIG. 5. Projection plots in $B \to K^{\pm}\pi^{\mp}$.

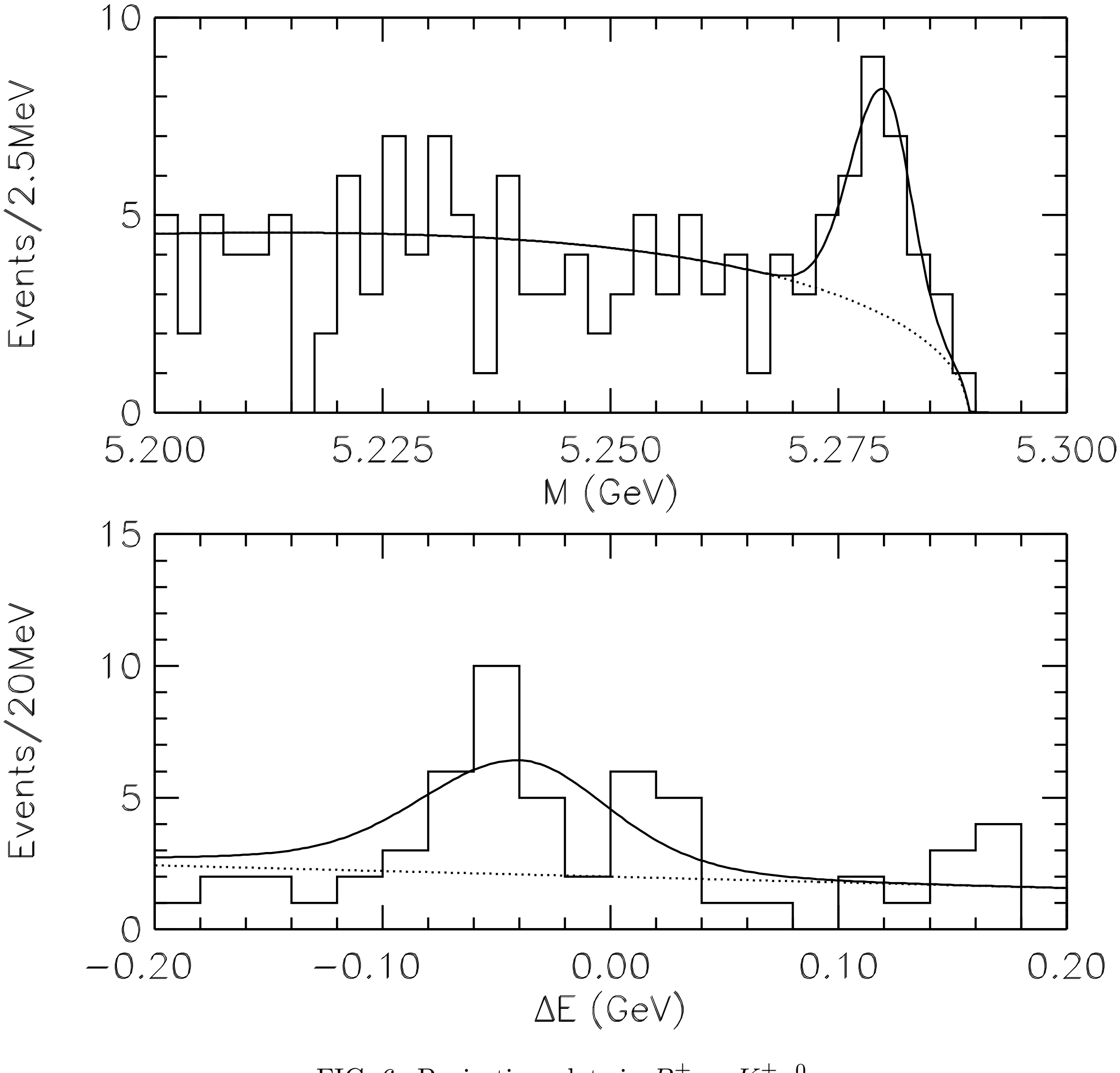

FIG. 6. Projection plots in $B^{\pm} \to K^{\pm}\pi^{0}$.

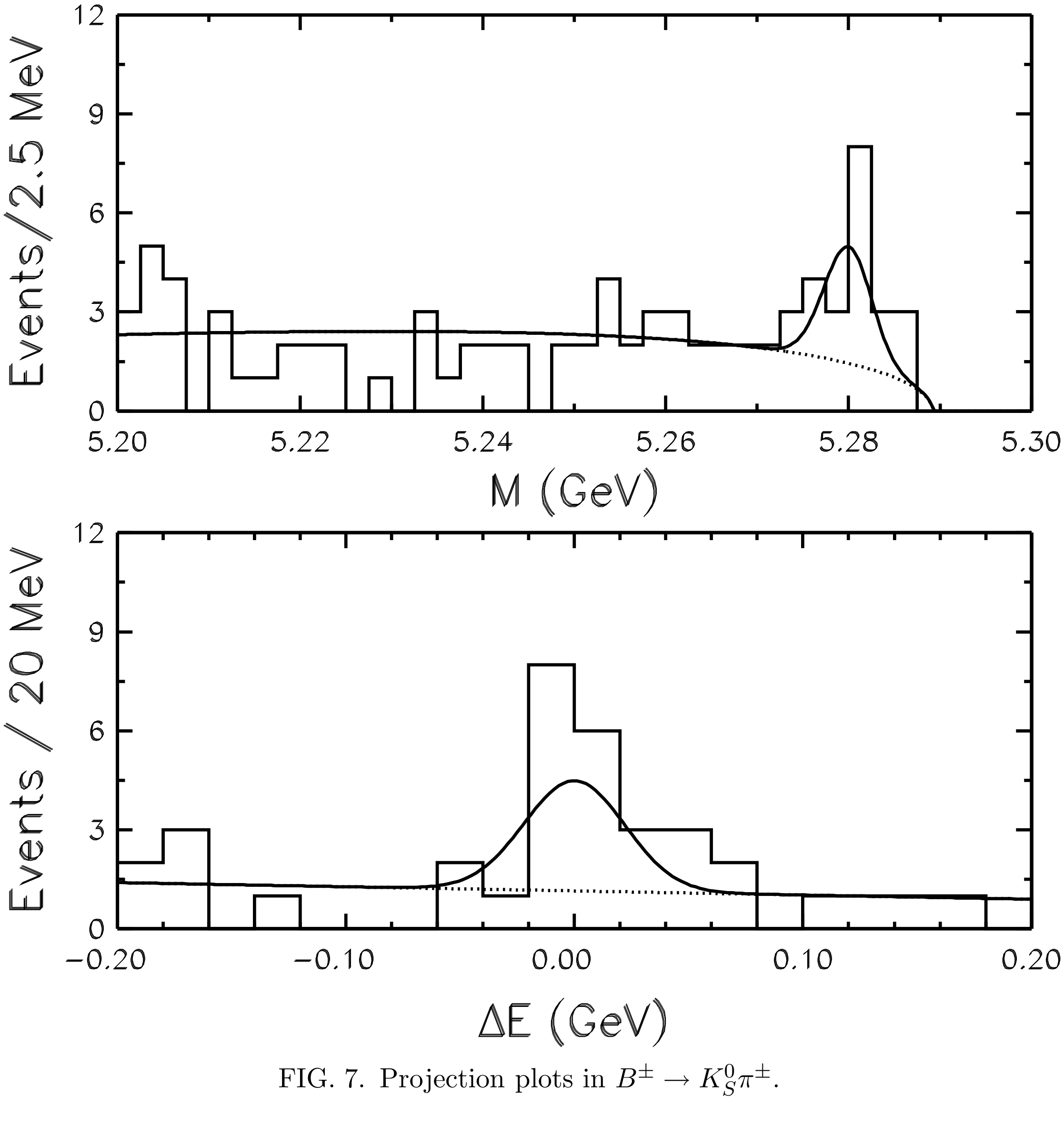

FIG. 7. Projection plots in $B^{\pm} \to K_S^0 \pi^{\pm}$.

In summary, we have measured branching fractions for three of the four exclusive $B \to K\pi$ decays, while only upper limits could be established for the processes $B \to \pi\pi, KK$. Our results therefore indicate that the $b \to sg$ penguin amplitude dominates charmless hadronic B decays. Furthermore, the 90% confidence level upper limit $\mathcal{B}(B \to \pi^+\pi^-) < 8.4 \times 10^{-6}$ does now rule out almost the entire range of theoretical predictions. However, one should note that all of these predictions assume constructive interference between the two isospin amplitudes [2]. A non-zero strong phase between these two amplitudes would reduce (enhance) the rate for $B \to \pi^+\pi^-(\pi^0\pi^0)$ and leave $B^\pm \to \pi^\pm\pi^0$ unchanged. Our limit on the latter has remained rather weak in comparison.

We gratefully acknowledge the effort of the CESR staff in providing us with excellent luminosity and running conditions. This work was supported by the National Science Foundation, the U.S. Department of Energy, Research Corporation, the Natural Sciences and Engineering Research Council of Canada, the A.P. Sloan Foundation, the Swiss National Science Foundation, and the Alexander von Humboldt Stiftung.

REFERENCES

[1] M. Kobayashi and K. Maskawa, Prog. Theor. Phys. **49**, 652 (1973).

[2] M. Gronau and D. London, Phys. Rev. Lett. **65**, 3381 (1990).

[3] M. Gronau, J. L. Rosner, and D. London, Phys. Rev. Lett. **73**, 21 (1994); R. Fleischer, Phys. Lett. B **365**, 399 (1996).

[4] R. Fleischer and T. Mannel, Phys. Rev. D **57**, 2752 (1998).

[5] J.-M. Gérard and J. Weyers, Université Catholique de Louvain preprint UCL-IPT-97-18(1997), hep-ph/9711469 (unpublished); M. Neubert, Phys. Lett. B **424**, 152 (1998). A. F. Falk, A. L. Kagan, Y. Nir, and A. A. Petrov , Phys. Rev. D **57**, 4290 (1998)

[6] R. Fleischer, CERN-TH/98-128, hep-ph/9804319 (unpublished); M. Gronau and J. Rosner, EFI-98-23(1998), hep-ph/9806348 (unpublished).

[7] R. Godang *et al.* (CLEO Collaboration), Phys. Rev. Lett. **80**, 3456 (1998).

[8] Y. Kubota *et al.* (CLEO Collaboration), Nucl. Instrum. Methods Phys. Res., Sec. A**320**, 66 (1992); T. Hill, 6th International Workshop on Vertex Detectors, VERTEX 97, Rio de Janeiro, Brazil.

[9] S. L. Wu, Phys. Rep. C**107**, 59 (1984).

[10] R. Brun *et al.*, GEANT 3.15, CERN DD/EE/84-1.

[11] D. M. Asner *et al.* (CLEO Collaboration), Phys. Rev. D **53**, 1039 (1996).

[12] G. Fox and S. Wolfram, Phys. Rev. Lett. **41**, 1581 (1978).

[13] N. G. Deshpande and J. Trampetic, Phys. Rev. D **41**, 895 (1990); L.-L. Chau *et al.*, Phys. Rev. D **43**, 2176 (1991); A. Deandrea *et al.*, Phys. Lett. B **318**, 549 (1993); A. Deandrea *et al.*, Phys. Lett. B **320**, 170 (1994); G. Kramer and W. F. Palmer, Phys. Rev. D **52**, 6411 (1995); D. Ebert, R. N. Faustov, and V. O. Galkin, Phys. Rev. D **56**, 312 (1997); D. Du and L. Guo, Zeit. Phys. C **75**, 9 (1997); N.G. Deshpande, B. Dutta, and S. Oh, hep-ph/9712445; H. Cheng and B. Tseng, hep-ph/9803457; A. Ali, G. Kramer, and C. Lü, hep-ph/9804363.